Research Article J. Electrochem. Sci. Technol., 2019, 10(2), 99-103

Naphthalene Derivative Supported Activated Carbon Composite Electrode with Enhanced Capacitance and Potential Window

Mengyang Hu, Jeong Ho Park*, Kwang Se Lee, and Jang Myoun Ko*

Department of Applied Chemistry & Biotechnology, Hanbat National University, San 16-1 Dukmyung-Dong, Yusung-Gu, Daejeon 305-719, Republic of Korea

ABSTRACT

A derivative of 1,4-Naphthoquinone coded HBU671 was synthesized and used in addition to activated carbon as composite electrode for supercapacitor application. From the electrochemical properties analysis, a specific capacitance of about 300 F g^{-1} exhibited almost two times of that of activated carbon at a scan rate of 100 mV s^{-1} and a potential window of - 0.2 - 1V. This improvement is due to the inherent redox reaction in HBU671. Cycle test also proved that this composite is still stable even after 1000 cycle within the applied potential window and it is highly recommended for practical application.

Keywords : Naphthoquinone, Organic additive, Composite electrodes, Supercapacitor

Received : 8 June 2018, Accepted : 1 October 2018

1. Introduction

Since the development of supercapacitor, its capacitance has never been enough to satisfy the continuous growing demands of industry. Researcheres want a better product to get better capacitance. Thus, various methods have been considered to improve its properties especially by increasing the capacitance. One of such ideas is the addition of different kinds of additives to the electrode material and evaluating any improvements made. Typically, metal oxides can contribute a lot to the capacitance, but their cost and availability restrict their use as commercial material [1,2]. Some organic compounds have also been tried as electrode additive; these include quinone, and their derivatives [3,4]. These have pseudo capacitance that occurs as a result of the hydroquinone-quinone redox reaction that increases the total specific capacitance [5,6]. Quinone is reduced to hydroquinone via incorporation of $2H^+$ with $2e^-$ during the discharging whereas hydroquinone is oxidized to quinone by generation of $2H^+$ with $2e^-$ during the charging as shown in Fig. 1(c) [7-13]. The quinone reaction is normally the most dominant when compared to other organic functionalities with pseudocapacitive reversible redox reactions.

In this study, a novel derivative 1,4-Naphthoquinone, 2-((4-(dimethylamino)phenyl) amino)naphthalene-1,4-dione (coded HBU671) is synthesized. The structure of the synthesized particles is shown in Fig. 1(a). The electrochemical properties of HBU671 are examined as pseudocapacitive additive for activated carbon electrodes. The contribution made by HBU671 on the activated carbon is mainly investigated in terms of specific capacitance, redox behavior and cycle life.

2. Experimental

2.1. Synthesis of HBU671

1,4-Dihydroxynaphthalene (100 mg, 1.0 eq) was dissolved in ethyl alcohol (23 mg, 0.1 eq). $CeCl_3 \cdot 7H_2O$ (101.9 mg, 1.2 eq) and N,N-Dimethyl-p-phenylenediamine (0.26 ml, 3.0 eq) was added with continuous stirring. Triethylamine was added in droplets and the mixture was stirred at room temperature for 24 hours. A solvent mixture of ethylacetate-hexane (1:1) is used for confirming the completion of the reaction by thin-layer chromatography (TLC). The product is

*E-mail address: jmko@hanbat.ac.kr, jhpark@hanbat.ac.kr

DOI: https://doi.org/10.5229/JECST.2019.10.2.99

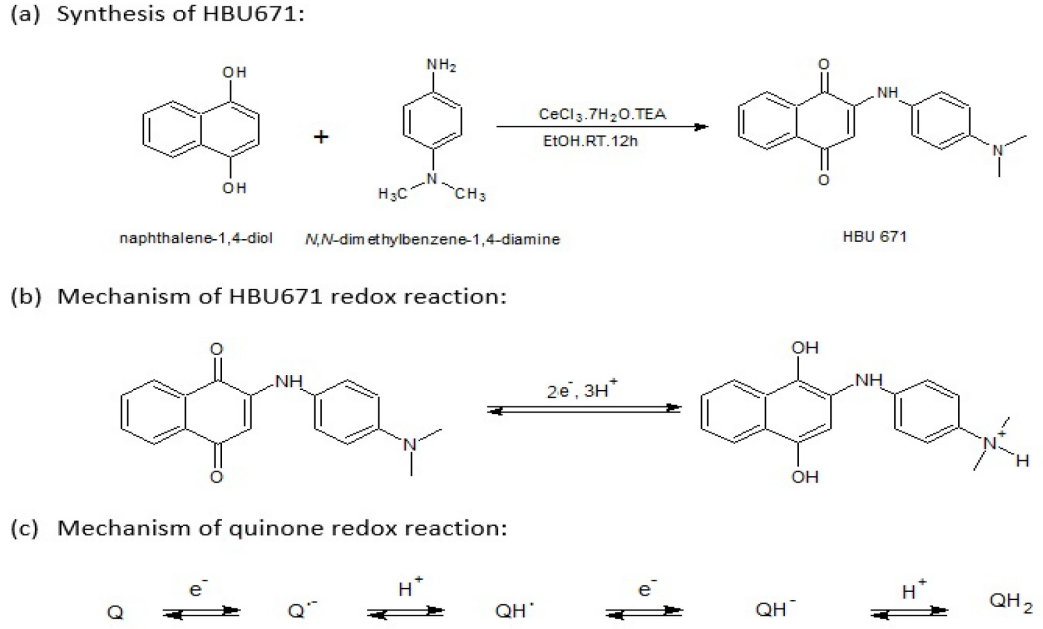

Fig. 1. (a) Synthesis of HBU671, (b) Mechanism of HBU671 redox reaction in electrode, and (c) Mechanism of redox reaction of quinone.

then recrystallized in water and finally dried at room temperature. The synthesized compound was coded HBU671 with a reaction yield of 80% and a melting point of 180°C. The structure of the synthesized compound was evaluated using proton nuclear magnetic resonance (1HNMR) spectroscopy (Varian Gemini 200NMR), which was identified as follows: 1HNMR (400MHz, DMSO) δ2.92 (s,6H), 5.92 (s,1H), 6.79 (d,J=8.8Hz,3H), 7.2 (d,J=8.4Hz,2H), 7.76 (t,J=7.2Hz,1H), 7.85 (t,J=7.2Hz,1H), 7.94 (d,J=7.2Hz,1H), 8.05 (d,J=7.6Hz,1H), 9.09 (s,1H).

2.2. Production of the Electrode

To prepare the electrode, activated carbon (MSC-30, specific surface area of 3000 $m^2 g^{-1}$, supplied by Kansai Cokes, 70 wt.%) as active material and HBU671 (25 wt.%) as organic additive was mixed in a mortar. 5 wt. % of poly (vinylidene fluoride) (Aldrich, MW=553,000) as a binder is dissolved in N-methyl-2-pyrrolidinone (NMP) as a dispersion solvent were added to form a slurry. The prepared slurry was coated on a platinum electrode surface which has a dimension of (1 cm × 1 cm) and dried at 80°C for at least 2 hours. For comparison, the same amount of the pure activated carbon and HBU671 were prepared using the same method. The infrared absorption spectra of activated carbon, HBU671 and their composite powders were obtained by Fourier-transform infrared spectroscopy (Bomem MB100). The surface morphologies of the produced electrodes were observed by using a thermal type field emission scanning electron microscope (Thermal type FE-SEM, Hitachi S-5000).

2.3 Electrochemical Analysis

Cyclic voltammetry measurement was conducted in a three-electrode cell compartment equipped with platinum as a counter electrode, the active material electrodes as the working electrode, and a reference electrode made up of Ag/AgCl saturated with KCl. The measurements were conducted in an electrolyte solution of 1M H_2SO_4, using an AUTOLAB Instrument (PGStat100, EcoChemie) at a potential range of -0.2 to 1.0 V vs. Ag/AgCl in a scan rate ranging from 100 to 1000 mVs^{-1}. Complex impedance spectroscopy was performed using a bias potential of 0.5 V to compare the electrical conductivity of the electrodes in 1M H_2SO_4. To compare the potential capacitances of the composite and activated carbon electrodes, charge-discharge cycle tests were also conducted at a

constant current density of 5.0 $mAcm^{-2}$. The specific capacitance (C) was calculated as a function of scan rate using the follow equation: $C=|qa+qc|/(2m\Delta V)$

Where q_a and q_c denote the anodic and cathodic charges on each scan, mass of the active material is represented as *m,* and ΔV denoted the potential window of the cyclic voltammetry.

3. Results and Discussion

The Fourier transform infrared spectroscopy (FT-IR) results of the activated carbon, HBU671, and their composite material are showed in Fig. 2. In this profile, there is a peak at about 3300 cm^{-1}. When compared to the structure of HBU671, (Fig. 1a), it coincides with the N-H group stretching in HBU671. Another important peak due to C=O group stretching from quinone is also found in the profile at about 1600 cm^{-1} [14]. Furthermore, the peaks from 700-1500 cm^{-1} are comparable to HBU-551 and HBU-552 [6] which have a similar structure to HBU671. However, the activated carbon sample did not possess any distinguished absorbance peaks in this wavenumber range. The above-mentioned peaks can also be found in the composite material, although they are not very obvious. That means the composite material has the adsorbed HBU671 in the pores of activated carbon which evaded detection by the FT-IR. This induced synergic effect was good for the composite due to the significant contributions made to the electrochemical performance by the HBU671.

Fig. 3 shows the surface images of activated carbon and the composite electrode. HBU671's solubility in NMP allows it to be mixed with activated carbon perfectly. While the NMP solvent is evaporated, the organic compound is deposited on the surface of the activated carbon and allow functional groups of HBU671 to create surface heterogeneity [15]. As shown in Fig. 3 (d), there are lots of small blocks which look like cauliflower stick within the bigger activated carbon blocks. The two particles blended perfectly, building good electric conductive network, since the HBU671 can partially fill the large pores and slits of activated carbon, to improve the capacitance of the whole electrode. Thus, the small particles which can be found in Fig. 3(d) as small sharp corner blocks are also connected to the system to improve the capacitance as a result of the organic compound bridges [5,6].

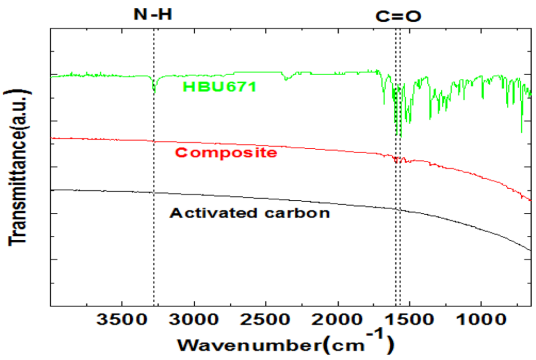

Fig. 2. Fourier-transform infrared spectra of the composite electrode, HBU671, and the activated carbon.

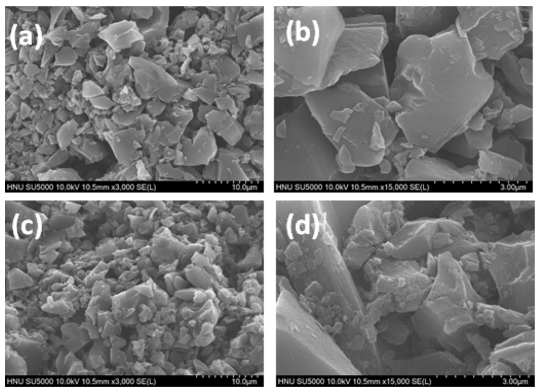

Fig. 3. Scanning electron microscopic surface images of the activated carbon (a,b) and composite electrode (c,d) at low and high magnification.

Fig. 4 shows the cyclic voltammograms of the composite electrode, activated carbon, and the HBU671. The redox reaction of the HBU671 is a two-step reaction occurring respectively at the position of the quinone group and amine group, as shown in Fig. 1b. HBU671 showed two set of redox peaks precisely at 0.11 V (anode)/ 0.01 (cathode) which can be ascribed to the quinone-hydroquinone redox transition and 0.75 V (anode)/ 0.64 (cathode) corresponding to the amine (–NH) group in the N, N-Dimethyl-p-phenylenediamine attached to the HBU671. These peaks are made pronounced in the composite electrodes, i.e. the activated carbon is able to influence the redox reaction in the composite electrode by accelerating the electron transfer process. The pristine activated carbon showed a typical electric double layer capacitor behavior compared to the composite. The graph also

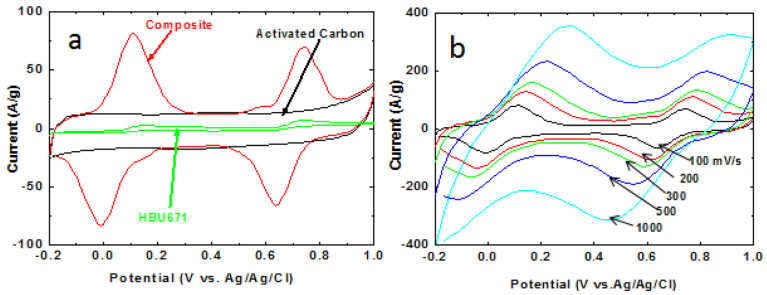

Fig. 4. Cyclic voltammograms of composite electrodes (a) compared with activated carbon at 100 mV s^{-1} and (b) at different scan rates.

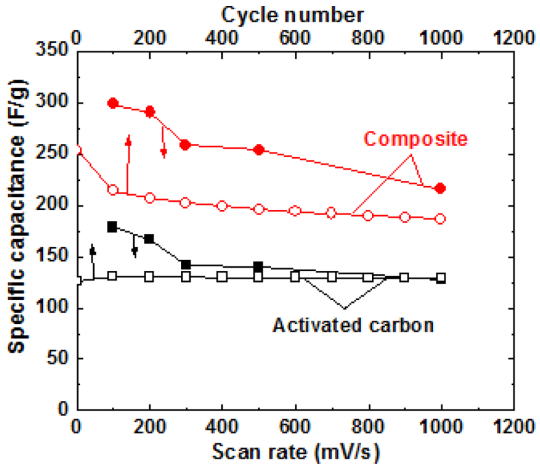

Fig. 5. Specific capacitances of the activated carbon and the composite electrodes as a function of scan rate and cycle number at 500 mV/s.

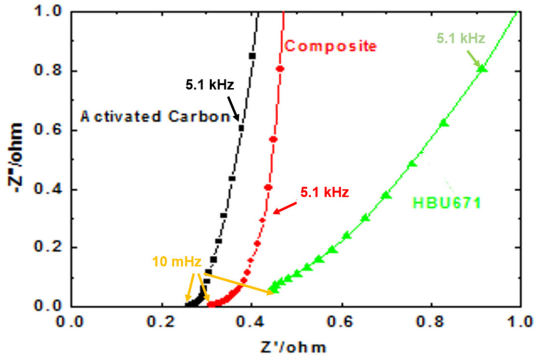

Fig. 6. Nyquist plots of activated carbon, HBU671, and the composite electrodes.

shows that beside the peaks, the composite material can also retain almost the same area to the activated carbon even though the percentage of activated carbon was decreased (see Fig. 4a). On the other hand, Fig. 4b shows that the reversibility of the composite is increased at a low scan rate but its reversibility decreases at a high scan rate. This is due to the slow ion diffusion; that is deviation from Nernstian behavior. This means the oxidation process in HBU671 occurs at the inner pore surfaces of the activated carbon and the reduction on its surfaces. This has also led to the shift in the peaks positions as the scan rate is increased.

Fig. 5 shows the specific capacitance as a function of scan rate and cycle number of the activated carbon and the composite electrodes. From the profile, a specific capacitance of 300 F/g was obtained for the composite electrode at a scan rate of 100 mV/s and a potential window of -0.2-1.0 V almost doubles that of the pristine activated carbon. Higher specific capacitances were obtained for the composite electrodes over the whole scan rate range compared to the pristine activated carbon. The enhanced capacitance can be ascribed to the additional redox reaction from the quinone and amine group in HBU671. The specific capacitance rapidly decreases within the first 100 cycles and finally a specific capacitance of 190 F g^{-1} was obtained after 1000 cycles. In spite of the decrease, the composite maintained higher specific capacitance compared to the activated carbon.

Fig. 6 shows the Nyquist plots for activated carbon, the HBU671, and the composite electrodes, which reflects the electrical conductivities of the electrodes. In these impedance spectra, their interfacial resistances become significant by the semicircles of the graphs, which are indicative of solid-like behaviors. Comparing the resistive behavior of the composite, activated carbon and the HBU671, it can be identified that the

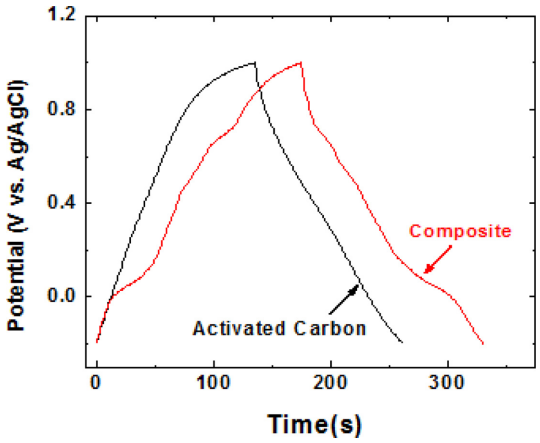

Fig. 7. Charge-discharge graphs of activated carbon and the composite electrodes, measured at 5.0 mA cm^{-2}.

resistive behavior of the composite falls between the activated carbon and HBU671, which further shows that mixing activated carbon and HBU671 facilitate the charge transfer in the redox reaction process in the composite electrodes. (See Fig. 3a).

In addition, Fig. 7 shows the charge-discharge profiles of the activated carbon and composite electrodes, recorded at a constant current density of 5.0 mA cm^{-2}, and a potential range of -0.2-1.0 V vs. Ag/AgCl. The average cycle time of the charge-discharge on the composite electrode is about 331 s, while the activated carbon electrode is 263 s. A longer charge-discharge time implies higher ability of electric energy storage. The enhanced charge-discharge cycle time of the composite is the result of the PhQ-$PhQH_2$ redox reaction complemented by the activated carbon, which accelerates this charge storage mechanism by creating a pathway for the transfer of ions and electrons.

4. Conclusions

In this study, a new derivative of 1,4-Naphthoquinone (HBU671) is chemically synthesized and added to activated carbon to make a composite electrode. The electrochemical properties thereof are studied for application in supercapacitors. The composite electrode demonstrated high specific capacitance of 300 Fg^{-1}; almost double that of pristine activated carbon in a potential window of -0.2-1.0 V at 100 mV s^{-1}. The increased capacitance of the composite electrodes benefits from HBU671's redox reaction at the quinone and amine groups attached to HBU671. The composite also demonstrated stable cycling performance at a higher scan rate. The low resistance and the intrinsic property of activated carbon accelerated the redox mechanism and provided stability to the HBU671 in the composite. These findings demonstrate that the derivatives of quinone can act as a very good additive to increase specific capacitance of activated carbon for supercapacitors.

Acknowledgment

This research was supported by a grant (10047758) from the Technology Development Program for Strategic Core Materials funded by the Korean Ministry of Trade, Industry & Energy.

References

[1] R. Kötz, M. Carlen, *Electrochim Acta*, **2000**, *45(15-16)*, 2483-2498.
[2] J-M. Ko, K-M. Kim, *Korean Chem. Eng. Res*, **2009**, *47*, 11-16.
[3] W. Lee, S. Suzuki, M. Miyayama, *Nanomaterials*, **2014**, *4(3)*, 599-611.
[4] M. Alejandro, I. Süheda, D. Raül, *Electrochemistry*, **2013**, *81(10)*, 853-856.
[5] J. H. Won, M. Latifatu, M. Jang, H. S. Lee, B. C. Kim, L. Hamenu, J. H. Park, K. M. Kim, J. M. Ko, *Synthetic Met*, **2015**, *203*, 31-36.
[6] H. S. Lee, M. Latifatu, B. C. Kim, J. H. Park, Y. G. Lee, K. M. Kim, J. W. Park, Y. G. Baek, J. M. Ko, *Synthetic Met*, **2016**, *217*, 29-36.
[7] M. Quan, D. Sanchez, M. F. Wasylkiw, D. K. Smith, *J Am Chem Soc*, **2007**, *129(42)*, 12847-12856.
[8] T. Kitagawa, X. Zhao, H. Imahori, C. Zhan, Y. Sakata, S. Iwata, *J. Phys. Chem. A*, **1997**, *101(4)*, 622-631.
[9] B. K. Jin, J. L. Huang, L. Li, S. Y. Zhang, Y. P. Tian, J. Y. Yang, *Anal. Chem*, **2009**, *81(11)*, 4476-4481.
[10] B. K. Jin, J. L. Huang, A. K. Zhao, S. Y. Zhang, Y. P. Tian, J. Y. Yang, *J. Electroanal. Chem*, **2010**, *650(1)*, 116-126.
[11] Y. Kim, Y. M. Jung, S. B. Kim, S. Park, *Anal. Chem*, **2004**, *76(17)*, 5236-5240.
[12] M. Bauscher, W. Mantele, *J. Phys. Chem*, **1992**, *96(26)*, 11101-11108.
[13] N. Gupta, H. Linschitz, *J Am Chem Soc*, **1997**, *119(27)*, 6384-6391.
[14] S. T. Senthilkumar, R. K. Selvan, N. Ponpandian, J. S. Melo, *RSC Adv*, **2012**, *2(24)*, 8937-8940.
[15] M. F. R. Pereira, S. F. Soares, J. J. M. Orfao, J. L. Figueiredo, *Carbon*, **2003**, *41(4)*, 811-821.